PAPER

Check for updates

Removal of manganous dithionate (MnS₂O₆) with MnO₂ from the desulfurization manganese slurry†

Lin Yang, [ID] *[ab] Cheng Wang,[a] Lu Yao, [ID] [ab] Wenju Jiang, [ID] *[ab] Xia Jiang [ID] [ab] and Jianjun Li[ab]

Manganese desulfurization has been increasingly explored, but the generated manganous dithionate (MD) by-product affects the valuable use of the desulfurized slurry. In this study, α-MnO₂, β-MnO₂, γ-MnO₂, and δ-MnO₂ were prepared for MD removal in desulfurization manganese slurry. Results showed that δ-MnO₂ had the best activity among the four because of its porosity and favorable surface properties. The operation conditions showed that 12.00 g L⁻¹ MD can be removed by more than 80.00% under the conditions of 1.4 mol L⁻¹ sulfuric acid, 100 g L⁻¹ δ-MnO₂ dosage, and reaction at 90 °C for 3 h. The MD removal with MnO₂ followed the decomposition–oxidation pass and direct oxidation–reduction reaction and consequently induced structure destruction and crystalline transfer. MD removal with natural MnO₂ ore was also examined, and natural MnO₂ ore in the δ type was found to have prominent activity. Thus, this type of natural MnO₂ may serve as a good alternative to pure MnO₂ for decreasing the cost of MD removal from desulfurization manganese slurry.
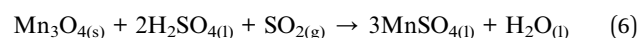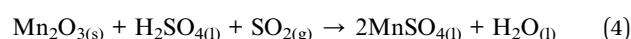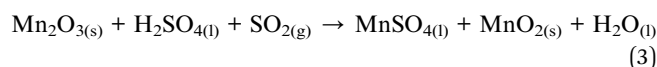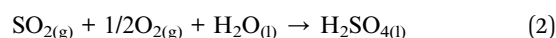
1. Introduction

Manganese is a strategic material applied in the metallurgical industry and for some nonferrous applications.[1] Traditional manganese metallurgy is a typical hydrometallurgical technology that generally involves ore milling, acid leaching, purification, and final electrowinning as the four main steps.[1,2] Given the sustained consumption of high-grade manganese ores, low-grade ore is increasingly being utilized. This condition causes the traditional hydrometallurgical process to be increasingly uncompetitive and uneconomical due to the increasing energy waste and serious environmental issue.

A new manganese-leaching method originally proposed for flue-gas desulfurization and for studying NO removal application has been developed, and thus provides a promising prospect for the manganese industry.[3–8] For flue-gas desulfurization, the commonly accepted reaction processes are expressed in eqn (1)–(6).[7,9,10] In these reactions, ores containing manganese oxide compounds (MnO₂, Mn₂O₃, Mn₃O₄) work as the active material to react with SO₂.

aCollege of Architecture and Environment, Sichuan University, Chengdu 610065, P. R. China. E-mail: andyyiyin@sina.com; wenjujiang@scu.edu.cn

bNational Engineering Research Center for Flue Gas Desulfurization, Sichuan University, Chengdu 610065, P. R. China
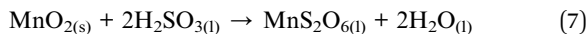
† Electronic supplementary information (ESI) available: Fig. S1: The XRD patterns of the α-, β-, γ- and δ-four different MnO₂; Fig. S2: The Mn 2p spectrum of α-, β-, γ- and δ-four different MnO₂; Fig. S3: The XRD pattern of the used natural MnO₂ ore; Table S1: The calculation of MD decomposition with different initial concentration, and the calculation method of MD concentration. See DOI: 10.1039/c9ra09810k

$$MnO_{2(s)} + SO_{2(g)} \xrightarrow{H_2O} MnSO_{4(l)} \qquad (1)$$

$$SO_{2(g)} + 1/2O_{2(g)} + H_2O_{(l)} \rightarrow H_2SO_{4(l)} \qquad (2)$$

$$Mn_2O_{3(s)} + H_2SO_{4(l)} + SO_{2(g)} \rightarrow MnSO_{4(l)} + MnO_{2(s)} + H_2O_{(l)} \qquad (3)$$

$$Mn_2O_{3(s)} + H_2SO_{4(l)} + SO_{2(g)} \rightarrow 2MnSO_{4(l)} + H_2O_{(l)} \qquad (4)$$

$$Mn_3O_{4(s)} + 2H_2SO_{4(l)} \rightarrow 2MnSO_{4(l)} + MnO_{2(s)} + H_2O_{(l)} \qquad (5)$$

$$Mn_3O_{4(s)} + 2H_2SO_{4(l)} + SO_{2(g)} \rightarrow 3MnSO_{4(l)} + H_2O_{(l)} \qquad (6)$$

During continuous SO₂ removal, ore manganese is leached to generate lixivium-containing MnSO₄, which is used for electrolytic manganese production (EMP). Compared with traditional acid leaching, desulfurization-based leaching omits sulfuric acid preparation and is energy saving because no calcination is required. Consequently, the technique renovation of manganese metallurgy industry may be greatly developed if traditional acid manganese leaching is replaced by manganese ore-based flue-gas desulfurization.

However, redox reaction between manganese oxide and SO₂, especially MnO₂, has the inevitable by-product manganous dithionate (MD), which is formed following 7 or 8 dues to incomplete oxidation.[10,11] MD significantly restrains electrowinning during EMP.[10,12] This process may be result in low product purity and some secondary pollution if the final product is MnSO₄. Therefore, the MD of manganese ore-based desulfurization must be managed to determine the economic value of this technology and further broaden its application.

$$MnO_{2(s)} + 2H_2SO_{3(l)} \rightarrow MnS_2O_{6(l)} + 2H_2O_{(l)} \quad (7)$$

or

$$MnO_{2(s)} + 2SO_{2(g)} \rightarrow MnS_2O_{6(l)} \quad (8)$$

A low MD concentration (<6 g L^{-1}) of desulfurized manganese slurry obtained may be due to the following two different aspects: (1) the formation suppression during desulfurization and (2) desulfurized slurry MD removal. Regulating the acidity of manganese slurry, inlet SO$_2$ concentration, and manganese composition can reduce MD formation.[13–15] However, we found that controlled MD formation is usually achieved at the expense of desulfurization performance and/or manganese leaching.[16] Consequently, a highly efficient MD removal method must be further explored.

Theoretically, MD can be decomposed into MnSO$_4$ and SO$_2$ at a relatively high temperature (>140 °C) or strong acid condition (eqn (9)).[4] Qu *et al.* studied manganese leaching with MnS$_2$O$_6$ and they found that S$_2$O$_6{}^{2-}$ can be somehow oxidized by MnO$_2$ (eqn (10)).[17] However, studies on the MD elimination using MnO$_2$ is still superficial, primarily focusing on the exploration of technical conditions. The reaction mechanism and kinetics remain unclear. Moreover, laboratory studies commonly use pure MnO$_2$. Thus, the significance of research results for industrial application remains to be verified.

$$MnS_2O_{6(l)} \rightarrow MnSO_{4(l)} + SO_{2(g)} \quad (9)$$

$$MnS_2O_{6(l)} + MnO_{2(s)} \rightarrow 2MnSO_{4(l)} \quad (10)$$
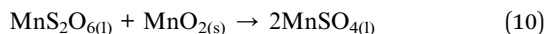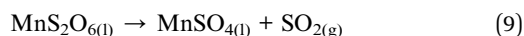
In this study, four types of MnO$_2$ with different crystalline structures were prepared by coprecipitation and hydrothermal methods to eliminate MD from desulfurized manganese slurry. The susceptibility and influences of MnO$_2$ crystalline, dosage, slurry acidity, and reaction temperature on MD removal were tested and discussed. The reaction mechanism of MD removal with MnO$_2$ was proposed on the basis of the experimental phenomenon and characterization before and after the reaction. Finally, the applicability of natural MnO$_2$ for MD removal was verified. The results showed good confirmation of the entire study.

2. Experimental

2.1 Materials and methods

MD-containing slurry was self-made using the pilot-scale system of manganese ore slurry-flue-gas desulfurization. The raw slurry had a pH of 1.6 and contained 15.35 g L^{-1} Mn^{2+} ion and 12.00 g L^{-1} MnS$_2$O$_6$. The KMnO$_4$ (AR), MnSO$_4$·H$_2$O (AR), (NH$_4$)$_2$S$_2$O$_8$ (AR), and H$_2$SO$_4$ (98%) were bought from Chron Chemicals (Chengdu, China) without further treatment.

Natural MnO$_2$ ore was shipped from the Gabonese Republic. Its main components based on the ICP-OES analysis after digestion are listed in Table 1.

2.2 Preparation of different MnO$_2$

α-MnO$_2$, γ-MnO$_2$, and δ-MnO$_2$ were prepared *via* coprecipitation. Specifically, 2.18 g of KMnO$_4$ (AR, Chron Chemicals, Chengdu, China) and 3.50 g of MnSO$_4$·H$_2$O (AR, Chron Chemicals) were dissolved in 50 mL of deionized (DI) water (the mole ratio of KMnO$_4$/MnSO$_4$·H$_2$O was 2/3). A new beaker was then preloaded with 100 mL of DI water and placed in an 80 °C water bath. The prepared MnSO$_4$ and KMnO$_4$ solutions were poured into the beaker at the same time, and the mixture was continuously mixed with a magnetic stirrer for 2 h. When the reaction process was completed, the obtained liquid–solid mixture was naturally cooled to room temperature and followed with repeated DI water washing until the pH of filtrate was almost 7. Finally, the mixture was dried at 80 °C for 12 h, and the obtained subparticle was the α-MnO$_2$. Compared with α-MnO$_2$ preparation, γ-MnO$_2$ synthesis involved a relatively lower thermostatic reaction temperature of 40 °C. For the preparation of δ-MnO$_2$, a different KMnO$_4$/MnSO$_4$·H$_2$O ratio of 4/3 was used. This solution was prepared with 2.18 g of KMnO$_4$ and 1.75 g of MnSO$_4$·H$_2$O dissolved in 50 mL of DI water and was used as reactants for the following synthesis process.

The hydrothermal method was used to prepare β-MnO$_2$ by using the precursors MnSO$_4$·H$_2$O and (NH$_4$)$_2$S$_2$O$_8$ (AR, Chron Chemicals). First, 8.45 g of MnSO$_4$·H$_2$O and 11.41 g of (NH$_4$)$_2$S$_2$O$_8$ were separately dissolved in 80 mL of DI water as substitute solution. For β-MnO$_2$ preparation, MnSO$_4$·H$_2$O solution was slowly instilled into (NH$_4$)$_2$S$_2$O$_8$ and allowed to react for 20 min with continuous magnetic stirring. Subsequently, the mixture was transferred to PTFE jars and subjected to a 12 h hydrothermal reaction at 140 °C. Subsequently, the mixture was naturally cooled to room temperature, and the following treatments, including filtration, washing, and drying, were performed similar to the coprecipitation method.

2.3 Removal of MD

Approximately 50 mL of desulfurized solution was placed into a 100 mL conical flask and then added with the calculated volume of sulfuric acid and MnO$_2$ or manganese ore. The flask was sealed with parafilm and placed in a thermostatic water bath for MD removal with continuous magnetic stirring. When the reaction was completed, the reaction mixture was rapidly filtered, and the MD concentration of the filtrate was measured to calculate the removal efficiency of MD (eqn (11)), where η (%) is the of MD removal efficiency, and C_0 and C_i (g L^{-1}) are the initial and final MD concentrations, respectively.

MD concentration before and after the removal reaction was determined by the distillation-iodometric method with some improvements.[18] Specifically, 1.0 mL of the filtrate was placed into a triangular flask and then added with 10.0 mL of 1+1 H$_2$SO$_4$. The flask was heated for distillation until acid mist formed and then cooled down naturally. The two-stage standard

Table 1 Analysis of the natural manganese ore used (wt%)

Components	Mn	Ca	Mg	Co
Content	40.35	0.72	3.41	0.025
Components	Ni	Zn	Fe	Cu
Content	0.025	0.001	0.010	0.0032

iodine solution (0.0100 ± 0.0005 mol L^{-1}) was used for SO_2 adsorption, and highly pure nitrogen gas was used as carrier gas during the entire distillation. After the entire reaction, residual iodine was titrated using standard sodium thiosulfate (0.0100 ± 0.0005 mol L^{-1}). To calculate MD concentration, a blank test was needed, which involved the use of the same volume of DI water in place of the sample. The blank was subjected to the same treatment and titration. For the blank test, the titration volume of sodium thiosulfate was V_0 (mL), and the volume of sodium thiosulfate used for the sample titration was V_1 (mL). The concentration of MD was calculated as in eqn (12), where C_{MD} is the concentration of MD (g L^{-1}), V is the sample volume used for test (mL), c is the concentration of sodium thiosulfate (mol L^{-1}), and m is the molar mass of MD (215.07).

$$\eta = \frac{C_0 - C_i}{C_0} \times 100\% \qquad (11)$$

$$C_{MD} = \frac{(V_0 - V_1) \, cm}{2V} \qquad (12)$$

2.4 Characterization

The crystallographic form of the prepared MnO_2 and natural manganese ore was analysed using an X-Pert PRO MPD diffractometer (Panalytical, NL) employing Cu Kα radiation at 30 kV and 20 mA. The step-scanning run over 2θ ranged at 10–80°, and crystalline phases were identified by the reference data from the International Center for Diffraction Data (JCPDs). Scanning electron microscopy (JEOL 7100F, Japan) with an acceleration voltage of 15.0 kV was used for the morphology characterization of the prepared MnO_2. SEM images with different magnifications were captured to obtain as much information as possible. X-ray photoelectron spectroscopy (XSAM-800, Kratos Co., UK) with Al (1486.6 eV) under ultra-high vacuum at 12.0 kV and 15.0 mA was applied to determine MnO_2 surface chemistry before and after MD removal. Energy calibration was performed by recording the core level spectra of Au $4f_{7/2}$ (84.0 eV) and Ag $3d_{5/2}$ (368.30 eV).

3. Results and discussion

3.1 MnO_2 preparation and characterization

Fig. 1 presents the SEM images of the prepared four different MnO_2. α-MnO_2 showed a homogeneous nanorod structure with a length of approximately 200–400 nm. β-MnO_2 represented a similar structure to that of α-MnO_2, but its diameter was relative larger and the length extended to range of 600–800 nm. In contrast with the above two compounds, γ-MnO_2 and δ-MnO_2 resembled a nanosphere structure. γ-MnO_2 nanosphere ranged from 200 nm to 500 nm in diameter and seemed to be assembled by organized short cylindrical nanorods radiating outward. The δ-MnO_2 sphere was likely to be constructed by a multi-layer nanowire, and the sphere diameter was relatively large ranging at approximately 500–800 nm. The morphology characterization of the prepared MnO_2 was consistent with that in previous studies,[19,20] confirming the preparation method used in this study. The XRD patterns in the Fig. S1† confirmed the classification, and the patterns of α-MnO_2, β-MnO_2, γ-MnO_2, and δ-MnO_2 were highly concordant with their reference data JCPDS 44-0141 (α-MnO_2), JCPDS 24-0735 (β-MnO_2), JCPDS 14-0644 (γ-MnO_2), and JCPDS 80-1098 (δ-MnO_2).[21–23]

To identify the composition and surface chemistry, we carried out X-ray photoelectron spectroscopy (XPS) characterization of all four types of MnO_2. Fig. S2† shows the high-resolution Mn 2p spectrum, and the Mn $2p_{3/2}$ characteristic peaks located close to 642.0 eV. This result identified that the manganese is typically Mn(IV)O_2, even though some differences occurred causing energy peak shift.[23] Fig. 2 illustrates the high-resolution O 1s spectrum. The characteristic peaks with a binding energy range of 529–530 eV corresponded with the lattice oxygen (O_L). Peaks with 531–532 eV binding energies were assigned to the defect oxide or surface oxygen ions (O_A), and those higher than 533 eV were due to the adsorbed water (O_H).[23–25] Compared with that of the three other samples, the O 1s spectrum of β-MnO_2 showed a shift to the relatively lower binding energy region, which may be attributed to hydrothermal reaction and is commonly observed in previous
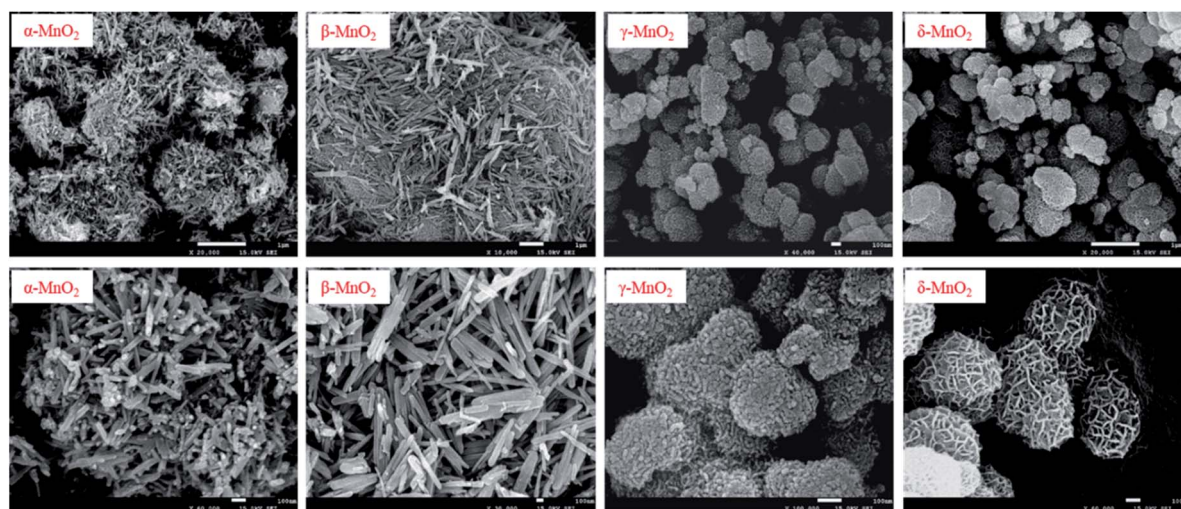

Fig. 1 SEM images of the MnO_2 prepared with different crystalline.

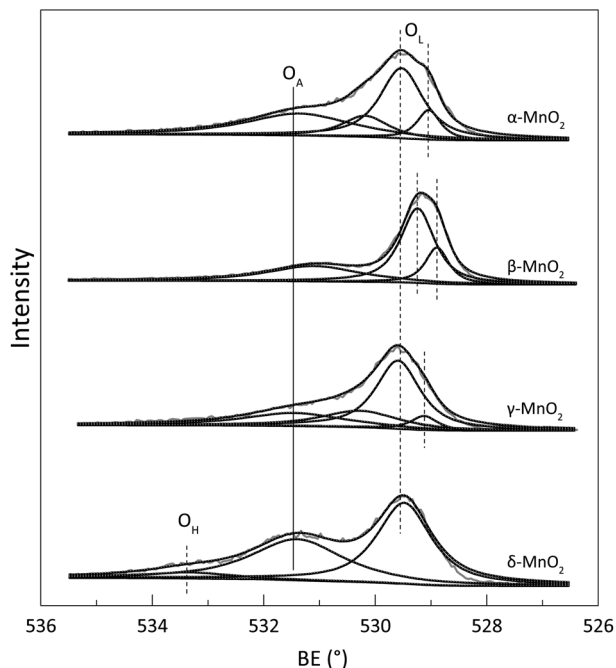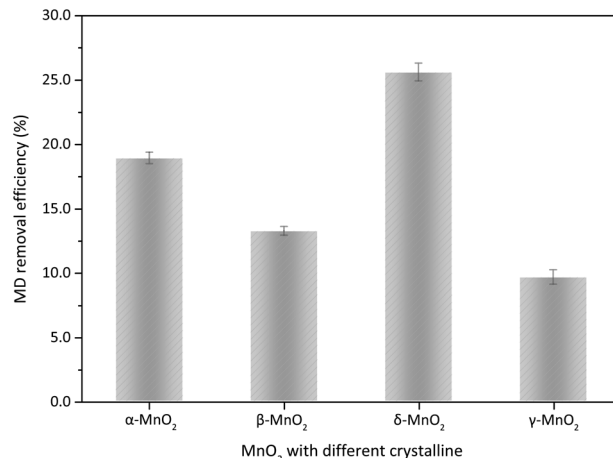Fig. 2   The O 1s spectrum of the prepared α-, β-, γ- and δ-MnO$_2$.

Fig. 3   The MD removal with different type of MnO$_2$ (reaction conditions: 8.00 g L^{-1} MD, 1.4 mol L^{-1} sulfuric acid, 100 g L^{-1} of MnO$_2$ addition, reacted at 60 °C for 3 h).

works.[23,26] Table 2 lists the O$_A$ contents of the α-, β-, γ-, and δ-MnO$_2$, which were 46.96%, 29.74%, 42.67%, and 43.32%, respectively. Theoretically, a high content of surface O$_A$ indicates that the sample has strong oxidizability because of its high mobility for the potential oxidation reaction.[27] Thus, the oxidation susceptibility of the four types of MnO$_2$ followed the order α-MnO$_2$ > γ-MnO$_2$ > δ-MnO$_2$ > β-MnO$_2$. Notably, the liquid–solid reaction was a multi-factorial process. Thus, effective contact surface area and interfacial mass transfer and must be analysed to make a comprehensive conclusion.

3.2   MD removal with different MnO$_2$

Fig. 3 demonstrates the activity of four different MnO$_2$ for the MD removal from the true desulfurized manganese slurry. The activity of four different MnO$_2$ used for the MD removal followed the sequence δ-MnO$_2$ > α-MnO$_2$ > β-MnO$_2$ > γ-MnO$_2$. δ-MnO$_2$ showed the best activity the MD oxidation under 1.4 mol L^{-1} sulfuric acid at 60 °C, with an MD removal efficiency of 25.63%.

Table 2   The surface oxygen chemistry based on the O 1s manipulation[a]

	O$_L$		O$_A$		O$_H$	
Samples	BE	%	BE	%	BE	%
α-MnO$_2$	529.04–529.53	53.05	530.18–531.36	46.96	NA	NA
β-MnO$_2$	528.89–529.24	70.26	531.10	29.74	NA	NA
γ-MnO$_2$	529.12–529.59	57.33	530.27–531.45	42.67	NA	NA
δ-MnO$_2$	529.48	50.80	531.40	43.32	533.34	5.88

[a] NA: not detected.

The valence of sulphur in MD is a transient state V, S$_2$O$_6$$^{2-}$ removal with MnO$_2$ is an oxidation process, and the activity of surface oxygen directly relate to the removal performance. As shown in Table 2, the O$_A$ content of four different MnO$_2$ followed the order β-MnO$_2$ < γ-MnO$_2$ < δ-MnO$_2$ < α-MnO$_2$. If the surface O$_A$ of MnO$_2$ is key factor to MD removal, α-MnO$_2$ should show the relatively best and β-MnO$_2$ exhibit the relatively worst MD removal performance. As shown in Fig. 3, the δ-MnO$_2$ demonstrated relative lower surface O$_A$ compared with α-MnO$_2$, while it showed the highest MD removal efficiency. This finding indicates that surface O$_A$ content was not the limiting factor for MD removal of four different MnO$_2$, it should be the effective surface area and/or interfacial mass transfer, which greatly affected the activity of MD removal.

MnO$_2$ with different crystallographic structures show different tunnel structures; α-MnO$_2$ and β-MnO$_2$ have [2 × 2] and [1 × 1] 1D tunnel structures, respectively; γ-MnO$_2$ has [1 × 1] and [1 × 2] alternating 1D structure, and α-MnO$_2$ has a layered structure.[19,28] For the three types of 1D structure MnO$_2$, their average chemical binding of Mn–O were 1.98 Å (α-MnO$_2$), 1.88 Å (β-MnO$_2$) and 1.91 Å (γ-MnO$_2$).[23] This finding indicates that α-MnO$_2$ has the best surface oxygen mobility among the structures.[29] Moreover, the [2 × 2] tunnel structure has stronger oxidation susceptibility than the [1 × 1] 1D tunnel structure.[23,30] These findings, including the experimental results in this study, may be used to explain why δ-MnO$_2$ had relatively better activity for MD removal than γ-MnO, β-MnO$_2$ and γ-MnO$_2$. In contrast with α-, β-, and γ-MnO$_2$, δ-MnO$_2$ had a layered structure and showed a reticular, hollow nanosphere morphology (Fig. 1). Zhang et al. characterized δ-MnO$_2$, showing the relative largest BET surface area among the four types of MnO$_2$.[20,23] This result indicates that δ-MnO$_2$ may provide more contacted reaction surface area and much more active sites could be exposed for interfacial reaction compared with the other forms. Moreover, the detected surface O$_H$ forecasted that δ-MnO$_2$ had better hydrophilia, which results in better molecular diffusion and mass transfer in aqueous reaction system. Therefore, we can

conclude that the better MD removal performance of δ-MnO$_2$ is attributed to the synergy work of the relative high O$_A$ content, improved porosity, and hydrophilia.

3.3 Influences of reaction parameters

In this section, the δ-MnO$_2$ that has the best reaction activity was used to discuss the influences of operation parameters on MD removal, including the reaction temperature, duration time, sulfuric acid content, MnO$_2$ dosage and MD concentration.

3.3.1 Reaction temperature. The operation conditions, including initial MD concentration, sulfuric acid content, and δ-MnO$_2$ addition, were kept constant. The influence of reaction temperature on the MD removal was discussed. As shown in Fig. 4, MD removal efficiency gradually increased with increased reaction temperature, indicating that the temperature significantly affected MD removal. At 60 °C, 25.63% of MD decomposed after 3 h of reaction. This value increased to 95.07% with increased temperature to almost 100 °C. Under high reaction temperature, the high molecular kinetic energy of reactants increased the probability of effective collision. Moreover, the MD molecules will become unstable under high reaction temperature and is active to react with δ-MnO$_2$. Considering economy and practical operation, the optimum reaction temperature should be 90 °C, and more than 85.00% of the MD could be removed.

3.3.2 Duration time. The operation conditions, including initial MD concentration, sulfuric acid and δ-MnO$_2$ addition, and reaction temperature, were kept constant. The results confirmed that MD removal changed with duration time. As the reaction continued, MD concentration gradually decreased (Fig. 5). Only 51.68% of the MD could be decomposed within 1 h of reaction, and this value increased to 85.94% at 3 h reaction time. Further prolonged reaction time was not recommended even though the removal efficiency also further increased. The reduced reaction rate may be due to (1) decreased reactant
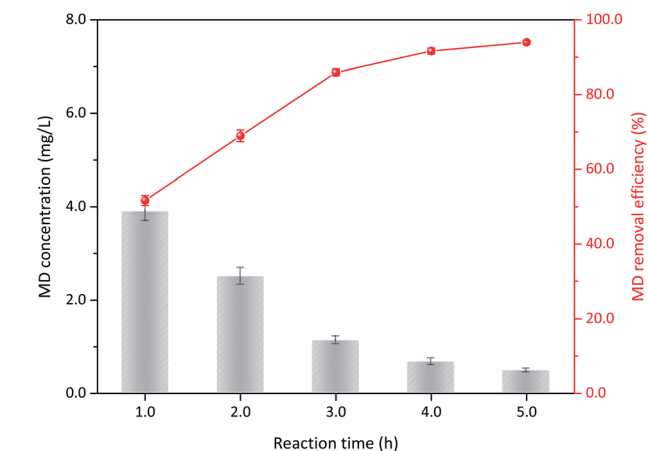
Fig. 5 The influence of reaction time on MD removal (reaction conditions: 8.00 g L^{-1} MD, 1.4 mol L^{-1} sulfuric acid, 100 g L^{-1} δ-MnO$_2$, reacted at 90 °C).

concentration and (2) the evolution of surface physicochemical properties.[31] With continuous reaction, the concentration of reactants gradually decreased, slowing mass transfer. Moreover, the reaction between the δ-MnO$_2$ and MD may also result in structure destruction and surface chemistry, such as layered structure, crystal structure, and composition of surface oxygen. δ-MnO$_2$ and MD worked synergistically to gradually reduce the reaction rate. Therefore, a too long reaction time only decreases production efficiency for industrial application. The recommend duration time is not more than 3 h.

3.3.3 Sulfuric acid concentration. The operation conditions, including initial MD concentration, δ-MnO$_2$ addition, and reaction temperature, was maintained constant to determine the effect of sulfuric acid addition on MD removal. At 1.0 mol L^{-1} acid concentration, the removal efficiency of MD was 61.34% after 3 h of reaction and only slightly increased at an acid content of 1.2 mol L^{-1} (66.32%, Fig. 6). Subsequently,
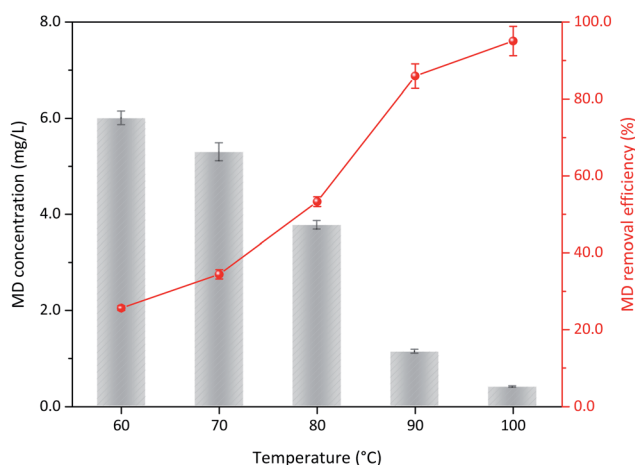
Fig. 4 The influence of reaction temperature on the MD removal with δ-MnO$_2$ (reaction conditions: 8.00 g L^{-1} MD, 1.4 mol L^{-1} sulfuric acid, 100 g L^{-1} δ-MnO$_2$, reacted 3 h).
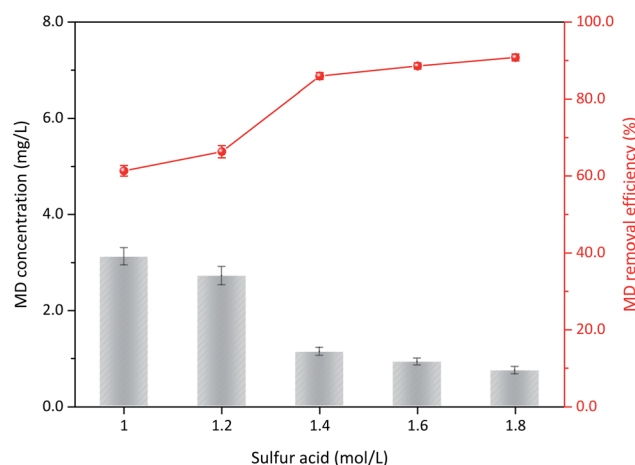
Fig. 6 The influence of sulfuric acid content on the MD removal (reaction conditions: 8.00 g L^{-1} MD, 100 g L^{-1} δ-MnO$_2$, reacted at 90 °C for 3 h).
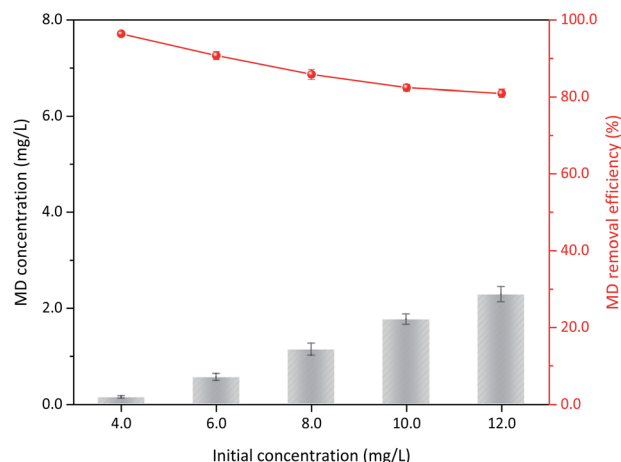
Fig. 7 The influences of initial MD concentration on MD removal (reaction conditions: 1.4 mol L^{-1} sulfuric acid, 100 g L^{-1} δ-MnO$_2$, reacted at 90 °C for 3 h).
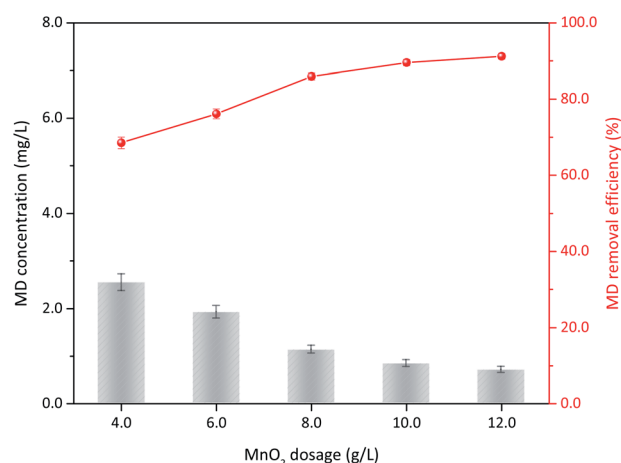

Fig. 8 The influences of δ-MnO$_2$ dosage on the MD removal (reaction conditions: 8.00 g L^{-1} MD, 1.4 mol L^{-1} sulfuric acid, reacted at 90 °C for 3 h).

MD removal efficiency increased with increased sulfuric acid content from 1.2 mol L^{-1} to 1.4 mol L^{-1}. The removal efficiency clearly increased from 66.32% to 85.95%. Subsequently, further addition of sulfuric acid addition was unnecessary, and the MD removal efficiency remained relatively stable. H$^+$ reportedly plays an important role in the δ-MnO$_2$ redox reaction, and a strong H$^+$ atmosphere can accelerate the oxidability of MnO$_2$.[32] For the MD removal using MnO$_2$, the MnO$_2$ was reduced to Mn^{2+}, and the redox potential between them ($E_{MnO_2/Mn^{2+}}$) could be calculated as in eqn (13).[32,33] Therefore, the increased acidity can promote the reduction potential of MnO$_2$, but a concentration higher than 1.4 mol L^{-1} is unnecessary.

$$E_{MnO_2/Mn^{2+}} = 1.229 - 0.118pH - 0.0296 \lg C_{Mn^{2+}} \qquad (13)$$

3.3.4 δ-MnO$_2$ dosage. The operation conditions, including initial MD concentration, sulfuric acid concentration, and reaction temperature, were kept constant. The influence of δ-MnO$_2$ dosage on the MD removal is illustrated in Fig. 7. When 60 g L^{-1} δ-MnO$_2$ was added, the MD concentration was reduced from 8.00 g L^{-1} to 2.54 g L^{-1}, showing 68.51% MD removal efficiency. The final concentration number decreased to 1.13 g L^{-1} (85.95%) with increased δ-MnO$_2$ to 100 g L^{-1}. Subsequently, only limited improvement was observed with further increased δ-MnO$_2$ dosage. With increased δ-MnO$_2$ addition, further active sites can participate to remove the MD, and a high MD removal efficiency is obtained.[34] Notably, the initial concentration of MD, acidity, and temperature were constant, which means MD could took part in the surface reaction had a maximum, excess δ-MnO$_2$ supply cannot improve the reaction efficiently. Consequently, 100 g L^{-1} δ-MnO$_2$ addition content for MD removal is recommended in this study.

3.3.5 Initial MD concentration. Sulfuric acid addition, δ-MnO$_2$ dosage, and reaction temperature were kept constant. Varied MD removal with initial concentration was also considered. Approximately 96.40% MD could be removed when the initial concentration was 4.00 g L^{-1}, and the apparent removal
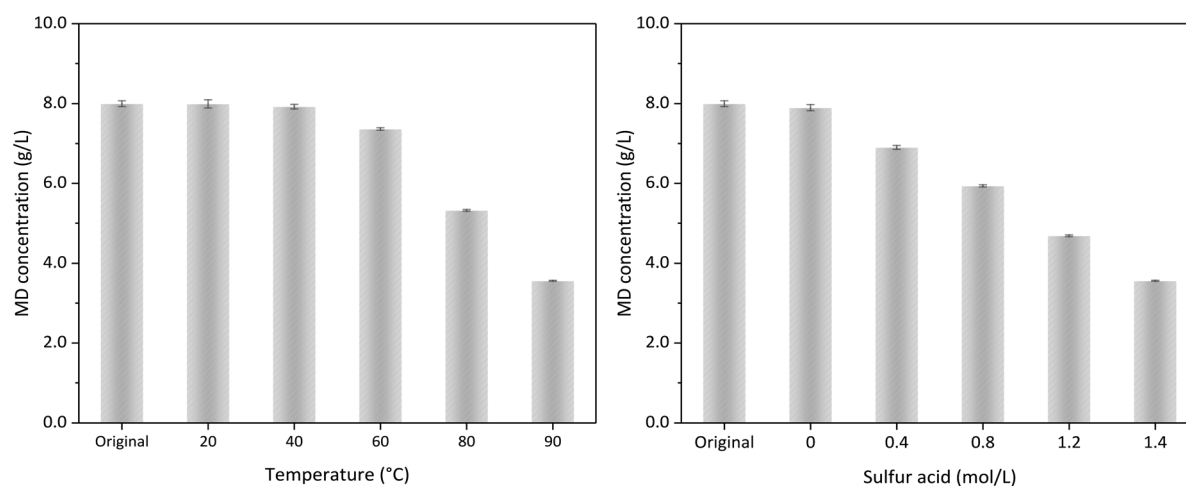

Fig. 9 The MD removal (a) in 1.4 mol L^{-1} sulfuric acid at different temperature, and (b) a constant temperature at 90 °C with different sulfuric acid dosage.

efficiency only showed a limited reduction with increased initial MD concentration (Fig. 8). Under the conditions of 1.4 mol L^{-1} sulfuric acid, 100 g L^{-1} δ-MnO$_2$ dosage, and 90 °C reaction temperature, up to 10.00 g L^{-1} MD could be reduced to less than 2.00 g L^{-1}. The corresponding removal efficiency was only decreased 15.44% to 80.96% when the initial concentration of MD increased three times to 12.00 g L^{-1}. This finding indicated that δ-MnO$_2$ had prominent stability and activity for MD removal under the optimized reaction conditions. Furthermore, the MD removed per unit δ-MnO$_2$ could be the best proof, which conspicuously raised from 38.6 mg L^{-1} g^{-1} to 97.1 mg L^{-1} g^{-1} δ-MnO$_2$ when the MD concentration was changed from 4.00 g L^{-1} to 12.00 g L^{-1} (Table S1†). The gradually reduced removal efficiency was attributed to the significant increase in initial MD concentration.

3.4 Mechanism analysis of MD removal

Fig. 9 shows the influence of temperature and acid concentration on the MD removal without δ-MnO$_2$ addition. Under 1.4 mol L^{-1} sulfuric acid and temperature higher than 60 °C, a part of MD could be decomposed without δ-MnO$_2$ addition. Fig. 4 reveals that δ-MnO$_2$ played a critical role for MD removal in the desulfurized manganese slurry. The influence of sulfuric acid content represented in Fig. 9b and 6 showed almost the same conclusion. Without any δ-MnO$_2$ addition, MD removal could be due to the MD self-decomposition under strong acidity condition. We found that the reaction products could discolour the C.1. Acid Violet 7 (18055) using the high-purity nitrogen as carry gas, which illustrated the formation of SO$_2$ in the strong acidity and high temperature condition (eqn (10)).

Fig. 10 shows the SEM images of δ-MnO$_2$ before and after MD removal. The uniform nanomesh-structure of δ-MnO$_2$ was clearly destroyed and presented a new analogous fusion surface after MD removal.[35] The destroyed structure followed clear agglomeration because the particle size of the used δ-MnO$_2$

residue was big. Fig. 11 illustrates the XRD patterns of the new δ-MnO$_2$ and reacted residue. The characteristic peaks belonging to δ-MnO$_2$ almost disappeared after MD removal. Alternatively, some characteristic peaks corresponding to α-MnO$_2$ were detected. This transformation indicated that MD removal resulted in the destruction of the 2D layered structure of δ-MnO$_2$ and consequently transferred to the [2 × 2] 1D α-MnO$_2$.[35] The MD removal shown in Fig. 3 indicates that the reaction activity of the four different MnO$_2$ structures followed order δ-MnO$_2$ > α-MnO$_2$ > γ-MnO$_2$ > β-MnO$_2$. This result indicates that the newly formed α-MnO$_2$ could remain effective for MD removal even though its activity is relative worse. This transformation of microcrystalline structure may also explain the influence of duration time shown in Fig. 5. The newly formed α-MnO$_2$ partially resulted in the gradually reduced reaction rate.

Based on the characterization, including SEM and XRD before and after the MD removal reaction, and considering previous results, the MD removal with MnO$_2$ may occur via the two following mechanisms. First is the decomposition–oxidation pathway (DO), in which MD is transferred to dithionic acid (H$_2$S$_2$O$_6$, eqn (14)) and then decomposed to H$_2$SO$_4$ and SO$_2$ (eqn (15)) the high temperature and strong acidity.[36] The generated SO$_2$ further reacts with MnO$_2$ to generate MnSO$_4$ (eqn (1)). Second is the direct oxidation–reduction (OR) reaction between the MD and MnO$_2$, which could be expressed by two half-reactions; the reduction half-reaction involves Mn(IV)O$_2$ obtaining two electrons to the divalent state (Mn(II)) (eqn (16)),[37] and the oxidation half-reaction involves S$_2$O$_6^{2-}$ donating electrons to SO$_4^{2-}$ (eqn (17)). The two half-reactions could be integrated into eqn (18), and its Gibbs free energy was calculated to be −279.70 kJ mol^{-1}.
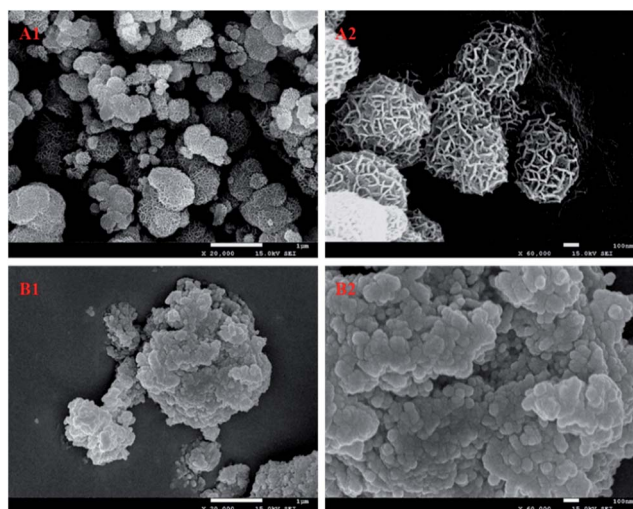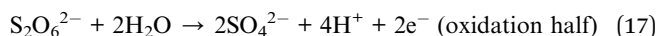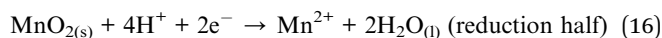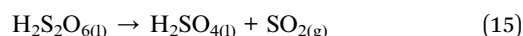
$$MnS_2O_{6(l)} + H_2SO_{4(l)} \rightarrow H_2S_2O_{6(l)} + MnSO_{4(l)} \quad (14)$$

$$H_2S_2O_{6(l)} \rightarrow H_2SO_{4(l)} + SO_{2(g)} \quad (15)$$

$$MnO_{2(s)} + 4H^+ + 2e^- \rightarrow Mn^{2+} + 2H_2O_{(l)} \text{ (reduction half)} \quad (16)$$

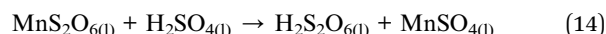$$S_2O_6^{2-} + 2H_2O \rightarrow 2SO_4^{2-} + 4H^+ + 2e^- \text{ (oxidation half)} \quad (17)$$

Fig. 10 The SEM image of δ-MnO$_2$ before (A1 and A2) and after (B1 and B2) the MD removal.
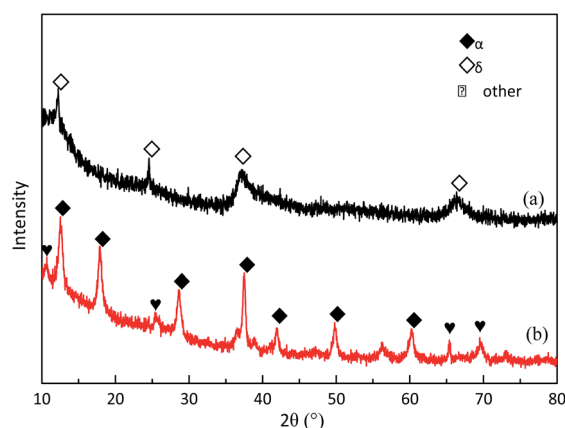

Fig. 11 The XRD patterns of δ-MnO$_2$ before (a) and after (b) the MD removal.
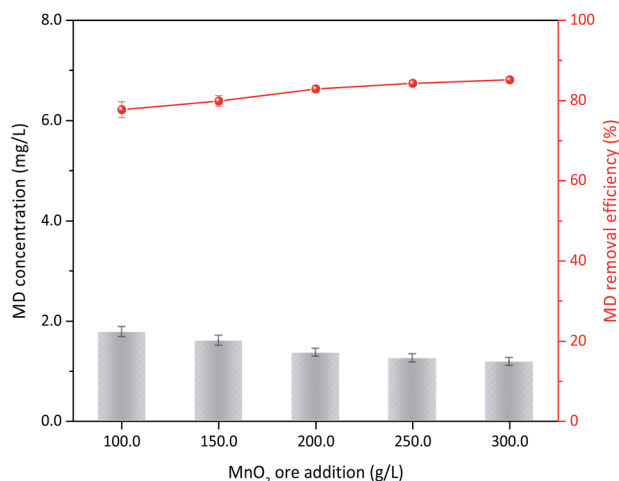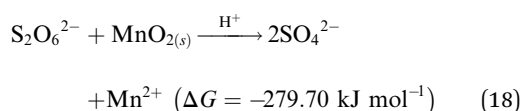
Fig. 12 MD removal with the natural MnO_2 ore (reaction conditions: 8.00 g L^{-1} MD, 1.4 mol L^{-1} sulfuric acid, reacted at 90 °C for 3 h).

$$S_2O_6{}^{2-} + MnO_{2(s)} \xrightarrow{\text{H}^+} 2SO_4{}^{2-}$$

$$+ Mn^{2+} \ (\Delta G = -279.70 \text{ kJ mol}^{-1}) \quad (18)$$

3.5 MD removal with natural manganese oxide ore

On the basis of the aforementioned results, MD removal with natural manganese oxide ore was carried out under relative optimum conditions. The XRD analysis indicated that MnO_2 in the ore was primarily the δ type (Fig. S3†), which had the best activity for MD removal among the four types of MnO_2 mentioned in this study. For the feasibility test, the operation conditions of 8.00 g L^{-1} MD, 1.4 mol L^{-1} sulfuric acid, 90 °C reaction temperature, and 3 h of reaction were used. MD removal at different ore dosages is shown in Fig. 12. MD removal showed a similar tendency with the synthesized δ-MnO_2. When 100 g L^{-1} ore were added, the final MD concentration was only 1.78 g L^{-1} (corresponded MD removal efficiency was 77.74%), which was even lower than the same content of pure δ-MnO_2 used. Increasing the dosage of MnO_2 ore slowly increased the removal efficiency. This finding indicated that natural MnO_2 ore is suitable for MD removal from desulfurization manganese slurry. In industrial applications, the desulfurization slurry should be further filtered before MD removal, and the MD removal residue can be returned to the front desulfurization section.

4. Conclusions

α-MnO_2, β-MnO_2, γ-MnO_2, and δ-MnO_2 were prepared for MD oxidation removal in desulfurized manganese slurry. Results showed that δ-MnO_2 had the best oxidation activity due to its porosity and favorable surface properties. The optimal conditions were 1.4 mol L^{-1} sulfuric acid, 100 g L^{-1} δ-MnO_2 dosage, and reaction at 90 °C for 3 h, which can remove more than 80.00% of MD with an initial MD concentration of 12.00 g L^{-1}.

The MD removal with MnO_2 followed the DO pass and direct OR reaction, and consequently induced structure destruction and crystalline transfer. MD removal with natural MnO_2 ore was also performed, and the natural MnO_2 ore in the δ type showed prominent activity. Thus, this type of natural MnO_2 ore can be a good alternative to pure MnO_2 for decreasing the cost of MD removal from desulfurization manganese slurry.

Conflicts of interest

There are no conflicts to declare.

Acknowledgements

References

1 K. Hagelstein, *J. Environ. Manage.*, 2009, **90**, 3736–3740.

2 N. Duan, Z. Dan, F. Wang, C. Pan, C. Zhou and L. Jiang, *J. Cleaner Prod.*, 2011, **19**, 2082–2087.

3 W. Sun, S. Su, Q. Wang and S. Ding, *Hydrometallurgy*, 2013, **133**, 118–125.

4 N. Chow, A. Nacu, D. Warkentin, H. Teh, I. Aksenov and J. W. Fisher, *Mining, Metallurgy & Exploration*, 2012, **29**, 61–74.

5 W. Ye, Y. Li, L. Kong, M. Ren and Q. Han, *Trans. Nonferrous Met. Soc. China*, 2013, **23**, 3089–3094.

6 W. Sun, S. Ding, S. Zeng, S. Su and W. Jiang, *J. Hazard. Mater.*, 2011, **192**, 124–130.

7 J. D. Miller and R. Wan, *Hydrometallurgy*, 1983, **10**, 219–242.

8 Y. Chen, Y. Li, X. Cao, J. Li, S. Tang, W. Ye and X. Zhang, *Korean J. Chem. Eng.*, 2019, **36**, 1082–1089.

9 Y. F. Li, H. Ye, C. Cao and L. N. He, *Adv. Mater. Res.*, 2011, **233–235**, 532–536.

10 Z. You, G. Li, Y. Zhang, Z. Peng and T. Jiang, *Hydrometallurgy*, 2015, **156**, 225–231.

11 R. E. Connick and Y. Zhang, *Inorg. Chem.*, 1996, **35**, 4613–4621.

12 C. B. Ward, *US Pat.* 7951282, 2011.

13 C. Ward, C. Cheng and M. Urbani, *Manganese-from waste to high-tech material*, Publications of the Australasian Institute of Mining and Metallurgy, 2004, vol. 2, pp. 241–246.

14 L. M. Petrie, *Appl. Geochem.*, 1995, **10**, 253–267.

15 Q. Wu, D. Zhang, P. Ning, J. Zhang, S. Li, C. Li and S. Wang, *Guangzhou Chem.*, 2017, **42**, 49–56, 73.

16 W. Zhang and C. Y. Cheng, *Hydrometallurgy*, 2007, **89**, 137–159.

17 B. Qu, L. Deng, B. Deng, K. He, B. Liao and S. Su, *React. Kinet., Mech. Catal.*, 2018, **123**, 743–755.

18 N. Soffer, *Analyst*, 1961, **86**, 843–849.

19 X. Wang and Y. Li, *J. Am. Chem. Soc.*, 2002, **124**, 2880–2881.

20 J. Zhang, Y. Li, L. Wang, C. Zhang and H. He, *Catal. Sci. Technol.*, 2015, **5**, 2305–2313.

21 B. Zhao, R. Ran, X. Wu and D. Weng, *Appl. Catal., A*, 2016, **514**, 24–34.

22 Y. Dong, H. Yang, K. He, S. Song and A. Zhang, *Appl. Catal., B*, 2009, **85**, 155–161.

23 S. Liang, F. Teng, G. Bulgan, R. Zong and Y. Zhu, *J. Phys. Chem. C*, 2008, **112**, 5307–5315.

24 Y. Dai, X. Wang, D. Li and Q. Dai, *J. Hazard. Mater.*, 2011, **188**, 132–139.

25 S. Ponce, M. A. Peña and J. L. G. Fierro, *Appl. Catal., B*, 2000, **24**, 193–205.

26 C. Yu, G. Li, L. Wei, Q. Fan, Q. Shu and J. C. Yu, *Catal. Today*, 2014, **224**, 154–162.

27 P. Gong, J. Xie, D. Fang, D. Han, F. He, F. Li and K. Qi, *Chin. J. Catal.*, 2017, **38**, 1925–1934.

28 Y. Ding, X. Shen, S. Gomez, H. Luo, M. Aindow and S. L. Suib, *Adv. Funct. Mater.*, 2006, **16**, 549–555.

29 J. Li, C. Song and S. Liu, *Acta Chim. Sin.*, 2012, **70**, 2347–2352.

30 T. Chen, H. Dou, X. Li, X. Tang, J. Li and J. Hao, *Microporous Mesoporous Mater.*, 2009, **122**, 270–274.

31 J. Klausen, S. B. Haderlein and R. P. Schwarzenbach, *Environ. Sci. Technol.*, 1997, **31**, 2642–2649.

32 H. Zhang and C. Huang, *Environ. Sci. Technol.*, 2005, **39**, 4474–4483.

33 A. T. Stone, *Environ. Sci. Technol.*, 1987, **21**, 979–988.

34 Z. He, L. Jiang, J. Chen and L. Zhang, *Shuichuli Jishu*, 2013, **39**, 34–39.

35 T. T. Truong, Y. Liu, Y. Ren, L. Trahey and Y. Sun, *ACS Nano*, 2012, **6**, 8067–8077.

36 R. Liang, S. Yao, C. Tang, S. Zhang and D. Hu, *J. Chongqing Univ.*, 1994, **17**, 88–92.

37 K. Lin, W. Liu and J. Gan, *Environ. Sci. Technol.*, 2009, **43**, 3860–3864.